PROCEEDINGS OF SCIENCE

Searches for lepton flavour/number violation in K^+ and π^0 decays at the NA62 experiment

Joel Swallow[†,*]

CERN,
Espl. des Particules 1, 1211 Meyrin, Switzerland

E-mail: joel.christopher.swallow@cern.ch

Searches for the lepton number violating $K^+ \to \pi^-\mu^+e^+$ decay and lepton flavour violating decays $K^+ \to \pi^+\mu^-e^+$ and $\pi^0 \to \mu^-e^+$ are reported, using NA62 data collected in 2017 and 2018. In the absence of a significant excess above the background in each channel, upper limits on the branching ratios are established at 90% confidence level: $\mathcal{B}(K^+ \to \pi^-\mu^+e^+) < 4.2 \times 10^{-11}$, $\mathcal{B}(K^+ \to \pi^+\mu^-e^+) < 6.6 \times 10^{-11}$, and $\mathcal{B}(\pi^0 \to \mu^-e^+) < 3.2 \times 10^{-10}$.

The 22nd International Workshop on Neutrinos from Accelerators (NuFact2021)
6–11 Sep 2021
Cagliari, Italy

[*]Speaker
[†]for the NA62 Collaboration:

A. Akmete, R. Aliberti, F. Ambrosino, R. Ammendola, B. Angelucci, A. Antonelli, G. Anzivino, R. Arcidiacono, T. Bache, A. Baeva, D. Baigarashev, L. Bandiera, M. Barbanera, J. Bernhard, A. Biagioni, L. Bician, C. Biino, A. Bizzeti, T. Blazek, B. Bloch-Devaux, P. Boboc, V. Bonaiuto, M. Boretto, M. Bragadireanu, A. Briano Olvera, D. Britton, F. Brizioli, M.B. Brunetti, D. Bryman, F. Bucci, T. Capussela, J. Carmignani, A. Ceccucci, P. Cenci, V. Cerny, C. Cerri, B. Checcucci, A. Conovaloff, P. Cooper, E. Cortina Gil, M. Corvino, F. Costantini, A. Cotta Ramusino, D. Coward, P. Cretaro, G. D'Agostini, J. Dainton, P. Dalpiaz, H. Danielsson, M. D'Errico, N. De Simone, D. Di Filippo, L. Di Lella, N. Doble, B. Dobrich, F. Duval, V. Duk, D. Emelyanov, J. Engelfried, T. Enik, N. Estrada-Tristan, V. Falaleev, R. Fantechi, V. Fascianelli, L. Federici, S. Fedotov, A. Filippi, R. Fiorenza, M. Fiorini, O. Frezza, J. Fry, J. Fu, A. Fucci, L. Fulton, E. Gamberini, L. Gatignon, G. Georgiev, S. Ghinescu, A. Gianoli, M. Giorgi, S. Giudici, F. Gonnella, K. Gorshanov, E. Goudzovski, C. Graham, R. Guida, E. Gushchin, F. Hahn, H. Heath, J. Henshaw, Z. Hives, E.B. Holzer, T. Husek, O. Hutanu, D. Hutchcroft, L. Iacobuzio, E. Iacopini, E. Imbergamo, B. Jenninger, J. Jerhot, R.W. Jones, K. Kampf, V. Kekelidze, D. Kereibay, S. Kholodenko, G. Khoriauli, A. Khotyantsev, A. Kleimenova, A. Korotkova, M. Koval, V. Kozhuharov, Z. Kucerova, Y. Kudenko, J. Kunze, V. Kurochka, V. Kurshetsov, G. Lanfranchi, G. Lamanna, E. Lari, G. Latino, P. Laycock, C. Lazzeroni, M. Lenti, G. Lehmann Miotto, E. Leonardi, P. Lichard, L. Litov, P. Lo Chiatto, R. Lollini, D. Lomidze, A. Lonardo, P. Lubrano, M. Lupi, N. Lurkin, D. Madigozhin, I. Mannelli, A. Mapelli, F. Marchetto, R. Marchevski, S. Martellotti, P. Massarotti, K. Massri, E. Maurice, A. Mazzolari, M. Medvedeva, A. Mefodev, E. Menichetti, E. Migliore, E. Minucci, M. Mirra, M. Misheva, N. Molokanova, M. Moulson, S. Movchan, M. Napolitano, I. Neri, F. Newson, A. Norton, M. Noy, T. Numao, V. Obraztsov, A. Okhotnikov, A. Ostankov, S. Padolski, R. Page, V. Palladino, I. Panichi, A. Parenti, C. Parkinson, E. Pedreschi, M. Pepe, M. Perrin-Terrin, L. Peruzzo, P. Petrov, Y. Petrov, F. Petrucci, R. Piandani, M. Piccini, J. Pinzino, I. Polenkevich, L. Pontisso, Yu. Potrebenikov, D. Protopopescu, M. Raggi, M. Reyes Santos, M. Romagnoni, A. Romano, P. Rubin, G. Ruggiero, V. Ryjov, A. Sadovsky, A. Salamon, C. Santoni, G. Saracino, F. Sargeni, S. Schuchmann, V. Semenov, A. Sergi, A. Shaikhiev, S. Shkarovskiy, M. Soldani, D. Soldi, M. Sozzi, T. Spadaro, F. Spinella, A. Sturgess, V. Sugonyaev, J. Swallow, A. Sytov, G. Tinti, A. Tomczak, S. Trilov, M. Turisini, P. Valente, B. Velghe, S. Venditti, P. Vicini, R. Volpe, M. Vormstein, H. Wahl, R. Wanke, V. Wong, B. Wrona, O. Yushchenko, M. Zamkovsky, A. Zinchenko.

© Copyright owned by the author(s) under the terms of the Creative Commons Attribution-NonCommercial-NoDerivatives 4.0 International License (CC BY-NC-ND 4.0).

PoS(NuFact2021)130

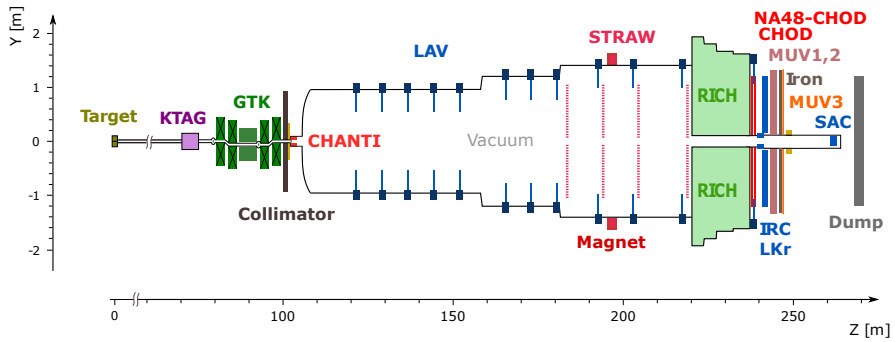

Figure 1: Schematic side view of the NA62 beamline and detector.

1. Introduction

In the standard model (SM) lepton number (LN) and lepton flavour (LF) numbers are conserved in interactions, corresponding to accidental global symmetries. However, their conservation is not imposed by any local gauge symmetry and in several beyond-the-standard-model (BSM) scenarios processes violating both LN and LF conservation are predicted to occur. Examples of such BSM scenarios are: LN violation via exchange of Majorana neutrinos [1], or LF violation via exchange of leptoquarks [2, 3], a Z' boson [4, 5] or in scenarios with light pseudoscalar bosons [6]. Observation of either LN or LF violating processes involving charged leptons would represent clear evidence for new BSM physics.

The NA62 experiment at the CERN SPS has collected the world's largest sample of K^+ decays, and a large sample of π^0 decays via the abundant $K^+ \to \pi^+\pi^0$ decay. This proceedings reports the searches performed, using NA62 data collected in 2017 and 2018, for the LN violating $K^+ \to \pi^-\mu^+e^+$ decay and LF violating decays $K^+ \to \pi^+\mu^-e^+$ and $\pi^0 \to \mu^-e^+$.

2. The NA62 experiment, data set and triggers

A schematic view of the NA62 beamline and detector is shown in Figure 1. In the following an overview of the main detectors used in the searches reported is provided, a complete description can be found in Ref. [7]. A 400 GeV proton beam from the SPS impinges on a berillyum target giving rise to a secondary hadron beam with a 6% component of K^+ with momentum 75 GeV/c. These K^+ are identified by a differential Cherenkov counter (KTAG) with a 70 ps resolution. A magnetic spectrometer (STRAW) measures the momenta and directions of charged particles produced in K^+ decays in a 75 m long fiducial volume (FV), 105–180 m downstream of the target. A ring-imaging Cherenkov detector (RICH) provides a trigger time with 70 ps precision. Particle identification for these searches is provided by a quasi-homogeneous calorimeter (LKr) and a muon detector (MUV3). A photon veto system includes the LKr and twelve ring-shaped lead-glass detectors (LAV1–12).

The data sample used for these searches corresponds to 8.3×10^5 SPS spills with a typical primary beam intensity of 2.2×10^{12} protons per spill of three seconds effective duration. The trigger system has a hardware level (L0) and a software level (L1). Three trigger chains were used to collect signal events: the multi-track (MT), electron multi-track (eMT), and muon multi-track (μMT) triggers. These triggers are typically downscaled by factors $D_{\mathrm{MT}} = 100$, $D_{e\mathrm{MT}} = 8$, and

PoS(NuFact2021)130

$D_{\mu\mathrm{MT}} = 8$, respectively, and are run concurrently with the experiment's primary trigger chain, dedicated to the measurement of the $K^+ \to \pi^+\nu\bar{\nu}$ branching ratio [8].

The MT trigger is a minimum-bias multi-track trigger, while the MTe and MTμ triggers include additional L0 conditions selecting multi-track events with at least one $e^\pm$ or $\mu^\pm$ candidate, respectively. Since $e^\pm$ deposit the majority of their energy in the LKr, the MTe trigger requires an LKr energy deposit of at least 20 GeV (LKr20 condition). The MTμ trigger requires a signal in the MUV3, as well as a 10 GeV LKr energy deposit (LKr10 condition). At L1 all three triggers require a K^+ candidate identified by the KTAG and a negatively charged particle track reconstructed in the STRAW. Additionally the MTμ trigger rejects events with signals in LAV stations 2–11.

3. Analysis strategy and event selection

The measurement of branching ratios for the signal channels are performed with respect to the normalisation channel $K^+ \to \pi^+\pi^+\pi^-$ ($K_{3\pi}$), and the MT trigger is used to collect $K_{3\pi}$ normalisation events. The event selection is described in Ref. [9] and briefly summarised below. Events are selected with three charged tracks forming a vertex with total charge +1 inside the FV. The total three-momentum at the vertex must be consistent with the beam momentum. Presence of a K^+ beam particle is required, identified by a KTAG signal consistent in time with the tracks. Events with LAV signals matched in time are rejected.

Normalisation $K_{3\pi}$ events are identified with reconstructed invariant mass, under the 3π mass hypothesis, consistent with the charged kaon mass within $3\sigma_{3\pi}$, where the measured mass resolution is $\sigma_{3\pi} = 0.9\ \mathrm{MeV}/c^2$. The normalisation channel selection acceptance is $A_n = 10.18\%$ [9].

The signal selection additionally applies particle identification (PID) criteria to the tracks. The PID conditions are based on the presence or absence of an associated MUV3 signal, and the E/p ratio, calculated from the energy (E) of the associated LKr cluster and the track momentum (p). The range of the vertex longitudinal position is optimised for signal channels to reduce the background from K^+ decays upstream of the FV. For the π^- channel selection, the mass of the π^-e^+ pair calculated under the e^-e^+ mass hypothesis is required to exceed $140\ \mathrm{MeV}/c^2$. This condition rejects backgrounds including π^0 with $\pi^0 \to e^+e^-\gamma$ decays and e^- misidentification as a π^-.

Signal is distinguished from background using the invariant mass, $m_{\pi\mu e}$, calculated assigning the π,μ,e masses to the tracks correspondingly identified by the PID criteria. The signal region is defined as 490–498 MeV/c^2, along with two $12\ \mathrm{MeV}/c^2$ wide control regions immediately above and below it (denoted CR1 and CR2 respectively). This 478–510 MeV/c^2 region was kept masked to avoid bias in the selection optimisation. The search for the decay chain $K^+ \to \pi^+\pi^0$ followed by $\pi^0 \to \mu^-e^+$, is performed using the sample of events passing the μ^- channel selection and requiring that the reconstructed mass of the μe pair is consistent with the π^0 mass, $|m_{\mu e} - m_{\pi^0}| < 2\ \mathrm{MeV}/c^2$. For the signal LN and LF violating modes simulations assuming uniform phase-space density are used for selection acceptance determination, and results are given in table 1.

4. Trigger Efficiency, normalisation and signal sensitivity

The efficiency for the trigger conditions is evaluated using minimum bias data. The efficiency of the MT trigger for normalisation events is $\varepsilon_{MT} = (93.2 \pm 0.5)\%$, with the equivalent result for

PoS(NuFact2021)130

Table 1: [9] Summary of inputs to the single event sensitivity calculation and corresponding resulting values for each search. The signal acceptances, A_s, are displayed with statistical uncertainties only; other uncertainties quoted are quadratic sums of the statistical and systematic uncertainties.

	$K^+ \to \pi^-\mu^+e^+$	$K^+ \to \pi^+\mu^-e^+$	$\pi^0 \to \mu^-e^+$
$A_s \times 10^2$	4.90 ± 0.02	6.21 ± 0.02	3.11 ± 0.02
$\varepsilon_{\mathrm{LKr10}} \times 10^2$	97.5 ± 1.3	97.5 ± 1.3	92.9 ± 1.2
$\varepsilon_{\mathrm{LKr20}} \times 10^2$	74.1 ± 1.6	73.3 ± 1.6	45.3 ± 1.0
$\mathcal{B}_{\mathrm{SES}} \times 10^{11}$	1.82 ± 0.08	1.44 ± 0.05	13.9 ± 0.9

signal-like events being consistent to within 1% [9]. For the MTe and MTμ triggers only the LKr20 and LKr10 conditions introduce non-negligible additional inefficiency, which depends on the total energy deposited in the LKr. Results are given in table 1.

The effective number of K^+ decays in the FV is $N_K = (1.33 \pm 0.02) \times 10^{12}$ [9]. The single event sensitivities, $\mathcal{B}_{SES}$, are defined for each process as the branching ratio corresponding to the observation of one signal event. Results are given in table 1.

5. Backgrounds

Backgrounds arise from particle misidentification and $\pi^\pm \to \ell^\pm\nu_\ell$ decays in flight of K^+ decay products. As an example, the largest background in the π^- channel signal region arises from $K^+ \to \pi^+e^+e^-$ decays where: the e^- is misidentified as a π^- (due to E/p mis-measurement) and either; a $\pi^+ \to \mu^+\nu_\mu$ decay in flight, or a π^+ is misidentified as a μ^+ (due to an accidental association with a MUV3 signal). In the μ^- channel the largest background is associated with $K_{3\pi}$ decays: this is due to a similar scenario of one π^+ misidentification as e^+ and one $\pi^+ \to \mu^+\nu_\mu$ decay in flight, but also from $K_{3\pi}$ decays upstream of the FV.

Background expectations are determined using simulations with data-driven corrections, assigning weights to each event accounting for misidentification probabilities and corrections for discrepancies between data and simulations. The background composition is similar in the control regions and signal region. The control regions were separately unmasked to validate the background prediction and the expected and observed numbers of events are largely consistent [9].

6. Results and conclusions

The mass spectra after unmasking for the π^- and μ^- channels are given in figure 2. The numbers of predicted backgrounds and observed events in the signal regions (SR) are given in table 2. Observed numbers of events are consistent with background predictions and upper limits (UL) on the branching ratios (at 90% CL) are established using the $\mathrm{CL_S}$ method [10], with results given in table 2. These results improve on previous searches [11] by one order of magnitude.

NA62 resumed data-taking in 2021 with new and upgraded detectors and beam-line configuration to assist with the primary objective of improving the precision of the study of the $K^+ \to \pi^+\nu\bar{\nu}$ decay [8].

PoS(NuFact2021)130

Table 2: Summary of results.

	$K^+ \to \pi^-\mu^+e^+$	$K^+ \to \pi^+\mu^-e^+$	$\pi^0 \to \mu^-e^+$
Predicted (SR)	1.07 ± 0.20	0.92 ± 0.34	0.23 ± 0.15
Observed (SR)	0	2	0
$\mathcal{B}$ UL@90%CL [$\times 10^{-11}$]	4.2	6.6	32

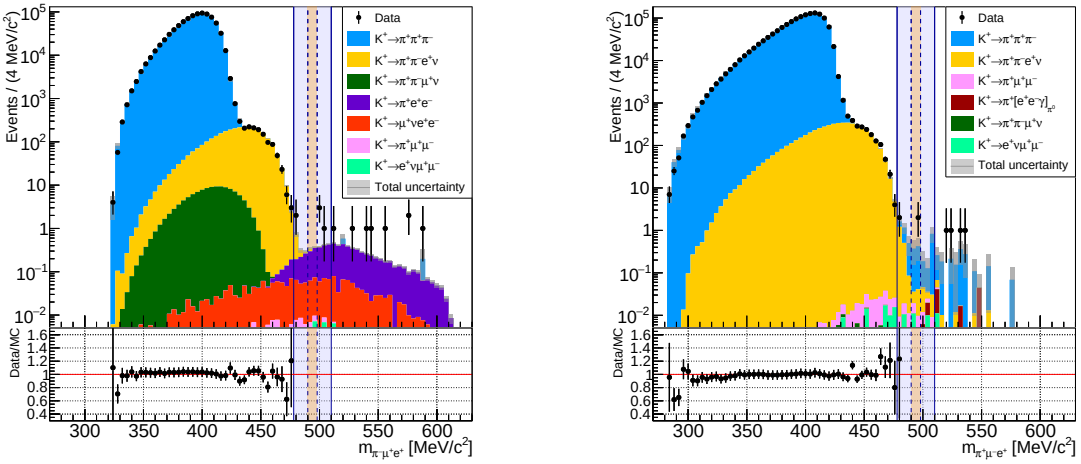

Figure 2: Reconstructed $m_{\pi\mu e}$ spectra for selected events, for data (black markers) and simulated background (filled areas) samples, in searches for $K^+ \to \pi^-\mu^+e^+$ (left) and $K^+ \to \pi^+\mu^-e^+$ (right). Lower panels show ratios between the observed numbers of data events and the predicted numbers of events from simulations.

References

[1] P. Minkowski *Phys. Lett. B* **67** (1977) 421.

[2] J. Pati and A. Salam *Phys. Rev. D* **10** (1974) 275.

[3] M. Bordone and others *J. High Energy Phys.* **10** (2018) 148 (2018).

[4] L.G. Landsberg *Phys. Atom. Nucl.* **68** (2005) 1190.

[5] P. Langacker *Rev. Mod. Phys.* **81** (2009) 1199.

[6] C. Cornella, P. Paradisi and O. Sumensari *J. High Energy Phys.* **01** (2020) 158 (2020).

[7] E. Cortina Gil and others *JINST* **12** (2017) P05025 (2017).

[8] E. Cortina Gil and others *J. High Energy Phys.* **06** (2021) 093.

[9] E. Cortina Gil and others *Phys. Rev. Lett.* **127** (2021) 131802.

[10] A. Read *J. Phys. G* **28** (2002) 2693.

[11] R. Appel and others *Phys. Rev. Lett.* **85** (2000) 2877.

PoS(NuFact2021)130